Implementing Innovative Ideas in Structural Engineering and Project Management
Edited by Saha, S., Zhang, Y., Yazdani, S., and Singh, A.

ISBN: 978-0-9960437-1-7

EXPERIMENTAL STUDY ON FLEXURAL BEHAVIOR OF STEEL-CONCRETE COMPOSITE BEAM COMPRISING PRECAST COMPOSITE SLABS

HETAO HOU[1], XIANG LIU[1], MINGYUAN FENG[1], LU GENG[2],
LEI CHEN[1], and HAINING LIU[1]

[1]*School of Civil Engineering, Shandong University, Jinan, P.R.China*
[2]*School of Civil Engineering, Shenyang Jianzhu University, Shenyang, P.R.China*

Four-point bending tests including twelve specimens were carried out to investigate the flexural rigidity, failure mode and ultimate capacity of the steel-concrete composite beam with a composite floor slab comprising 30 mm thick precast prestressed concrete panels and T-shaped concrete ribs (PPCRP). The test parameters included support length of PPCRP, thickness of the composite floor slab, longitudinal compressive reinforcement ratio, degree of the shear connection and the direction of T-shaped concrete rib. Strain distribution along the depth of mid-span section was obtained by strain gauges. Based on the moment-deflection curves of specimens, it was showed that flexural behavior of precast composite floor slab was similar to that of concrete floor slab cast in-situ during the elastic stage. Two failure phenomena were observed: i) Interface bond slip between the precast panel and the cast in-situ layer; ii) Diagonal shear crushing in one shear span. Compared with the floor slab cast in-situ, a slight decline in the ultimate flexural capacity was observed for the composite beam with composite floor slab. Analyses about the effects of all parameters on composite beams' rigidity and ductility were presented.

Keywords: Steel-concrete composite beam, Four-point bending test, Pre-cast floor slab with ribs, Flexural behavior.

1 INTRODUCTION

Steel-concrete composite beams have been widely used as a cost-effective structure style for floor systems in multi-story steel frame construction. The last two decades have seen the increasing use of precast hollow core slabs acting compositely with steel beams. Many experiments and finite element analyses on it have been carried out (Lam 2007 and Hegger 2009). Meanwhile, a recent development in China is the use of precast prestressed concrete panels with T-shaped concrete ribs (PPCRP) as both a permanent formwork and as a part of composite floor slab (Zhou 2006). Wu (2011) showed that PPCRP could satisfy the requirements of bearing capacity in construction phase and it behaved similarly to the cast-in-situ floor slab during the flexural experiment.

However, few experimental studies have investigated the composite action between the steel beams and composite floor slabs with PPCRP, which can yield a more efficient and rational design of composite beams. In this paper, four-point bending tests including twelve full-scale specimens were carried out. To investigate the factors which influenced the flexural behavior, test parameters included support length of PPCRP, thickness of the composite floor slab, longitudinal compressive reinforcement ratio, degree of the shear connection and the direction of T-shaped concrete rib.

2 EXPERIMENTAL PROGRAM

2.1 Specimen Design

All specimens' span length was 3000 mm with the same slab width of 800 mm. And the steel beams of the specimens were welded per Chinese standards, having a section of H200×150(100)×6×8. To validate that the PPCRP's arrangement had a significant impact on the flexural behavior, the support length, a, varied from 0mm to 60mm as a main parameter. Besides, the ribs' direction distinguished specimen SCB-11 from others for its ribs in a parallel, as opposed to vertical, position to the axis of steel beam.

As specified in the Chinese code (GB50017-2003), the degree of shear connection could be calculated as $\beta = n_r / n_s$, where n_r = actual number of studs in shear span; n_s = the number of studs to transfer all longitudinal shear force in shear span. Corresponding to different degrees of shear connection, the spacing of studs was 130 mm for most of specimens, 100 mm for SCB-7 and 150 mm for SCB-8. The studs needed were evenly arranged in the shear span, and extended throughout the pure bending zone. Figure 1 and Table 1 shows the main details of specimens.

Table 1. Testing Matrix.

Specimen	Type	Direction of ribs	h_c (mm)	a (mm)	s (mm)	β	ρ_l
SCB-1	composite	vertical	130	40	130	1.0	0.29% (12Φ8)
SCB-2	composite	vertical	140	40	130	1.0	0.27% (12Φ8)
SCB-3	composite	vertical	150	40	130	1.0	0.25% (12Φ8)
SCB-4	composite	vertical	130	0	130	1.0	0.29% (12Φ8)
SCB-5	composite	vertical	130	20	130	1.0	0.29% (12Φ8)
SCB-6	composite	vertical	130	60	130	1.0	0.29% (12Φ8)
SCB-7	composite	vertical	130	40	100	1.32	0.29% (12Φ8)
SCB-8	composite	vertical	130	40	150	0.86	0.29% (12Φ8)
SCB-9	composite	vertical	130	40	130	1.0	0.46%(12Φ10)
SCB-10	composite	vertical	130	40	130	1.0	0.65%(12Φ12)
SCB-11	composite	parallel	130	40	130	1.0	0.29% (12Φ8)
SCB-12	cast-in-situ	--	130	--	130	1.0	0.29% (12Φ8)

Note: h_c = thickness of floor slab, a = support length of PPCRP, s = spacing of headed shear studs, ρ_l = longitudinal compressive reinforcement ratio, β = degree of shear connection

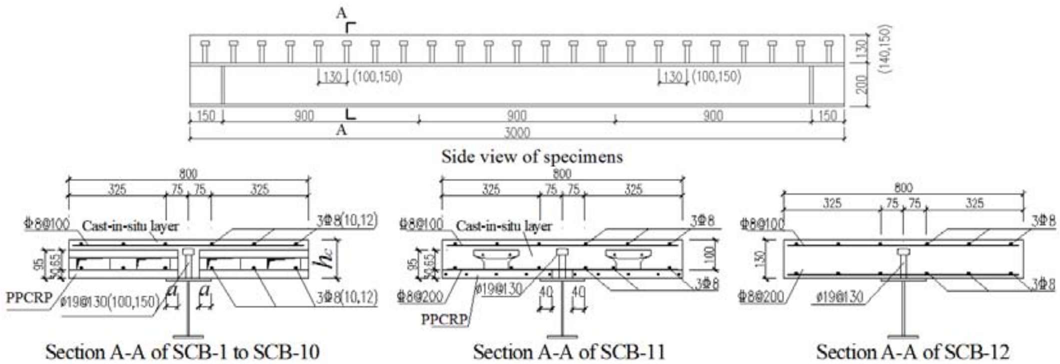

Figure 1. Sectional and reinforcement layout of specimens.

2.2 Specimen Construction and Material Strength

When arranged in a position with ribs vertical to the steel beam, six PPCRPs were needed for each specimen construction. Rebars with diameter of 8 mm were used as reinforcement in the cast-in-situ layer for both the longitudinal and transverse directions.

During slab concreting, six concrete cubes of 100 mm in side length were made and then tested in the laboratory according to Chinese standards, thus obtaining the cubic strength f_{cu} and the axial compressive strength f_c listed in Table 2. The yield strength of steel for steel beam was 360 MPa and the ultimate strength was 503 MPa.

Table 2. Mechanical properties of concrete (unit: MPa).

Concreting	Cubic strength f_{cu}	Axial compressive strength f_c	Elastic modulus E_c
PPCRP	53.2	34.05	3.51×10^4
Cast-in-situ layer	38.6	25.82	3.23×10^4

2.3 Test Procedure and Instrumentation

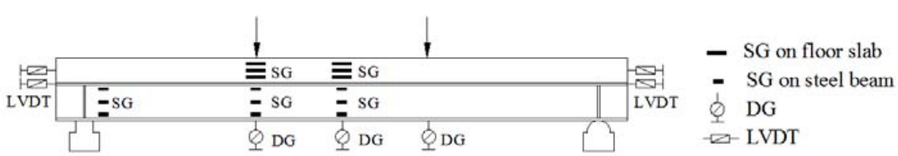

Figure 2. Location of strain gauges (SG), dial gauges (DG) and linear voltage displacement transducers (LVDT).

Every specimen was simply-supported and subjected to two-point monotonic loads by a hydraulic jack. The load was applied to the top surface of the slab through a distribution beam and two cross beams, thus generating shear spans near the beam ends and a pure bending zone in the middle, as shown in Figure 2. Each step of load increased by a tenth of ultimate load estimated and last for 5 minutes, which was controlled by a load cell. During the tests, the following quantities were monitored: deflection along the beam axis, relative slip at beam ends, strains in the steel beam and floor slab.

3 OBSERVATIONS AND FAILURE MODES

The loading response and the failure mode were similar for specimens with composite floor slabs as described in Figure 3. Under the initial load (43% M_{ut}) the mid-span deflection kept increasing with small cracks appearing in the gaps between PPCRPs. At $M = 132\ kN \cdot m$ (54% M_{ut}), the bottom flange of steel beam yielded and the first crack generally formed between cast-in-situ layer and precast panels. When the load reached 190 $kN \cdot m$ (78% M_{ut}), cracks along the interface propagated obliquely to the load point. At the collapse load, the debonding failure along the interface occurred within the range of 100 mm from the gaps between PPCRPs, which was then followed by a rapidly development of shear cracks. The resisting shear ability of composite slab declined after the debonding failure, thus generating the diagonal shear crushing in one shear span.

For the specimen SCB-12 with cast-in-situ floor slab, the failure mode consisted in the crushing of the floor slab's top layer after the tensioned steel yield at mid-span.

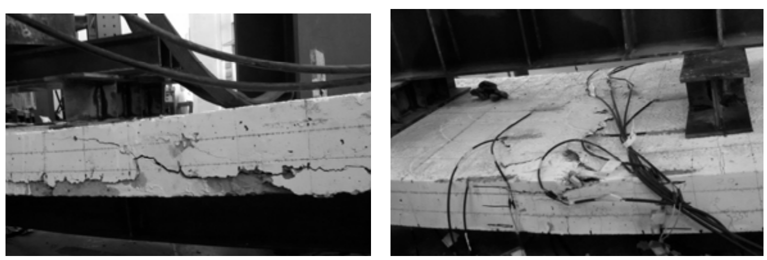

(a) (b)

Figure 3. Typical failure modes: (a) diagonal shear crushing for SCB-1 with composite floor slab and (b) crushing of concrete for SCB-12 with cast-in-situ floor slab.

4 EXPERIMENTAL RESULTS AND DISCUSSION

4.1 Primary Experimental Results

The test results for twelve specimens are summarized in Table 3, where M_{cr} = mid-span moment corresponding to the first crack; M_{yt} = mid-span moment corresponding to the first yielding of steel beam; M_{ut} = mid-span ultimate moment; δ_{yt} = mid-span deflection corresponding to M_{yt} and δ_{ut} = mid-span deflection corresponding to M_{ut} .

4.2 Moment-Deflection Response

Figure 4 shows $M-\delta$ (mid-span moment vs. mid-span deflection) curves for all the specimens, which can be divided into two phases: the elastic phase and the plastic phase. The $M-\delta$ curve for SCB-12 with cast-in-situ floor slab was nearly linear up to 57% M_{ut} . Above this load level, a reduction in rigidity was considerable but not rapid.

In comparison with SCB-12, however, there were differences in the ultimate moment value and the maximum mid-span deflection of composite beams with composite floor slabs. Initial imperfections, which existed in the gaps between PPCRPs, caused a slight decline in the flexural capacity but an obvious reduction in the maximum mid-span deflection. Furthermore, the specimen with composite floor slab had a flexural rigidity similar to that with cast-in-situ floor slab in the elastic phase.

Table 3. Experimental results of steel-concrete composite beams.

Specimen	$M_{cr}(kN\cdot m)$	$M_{yt}(kN\cdot m)$	$M_{ut}(kN\cdot m)$	$\delta_{yt}(mm)$	$\delta_{ut}(mm)$	M_{yt}/M_{ut}	δ_{ut}/δ_{yt}
SCB-1	112.5	132.5	247.1	6.38	41.83	0.54	6.56
SCB-2	121.5	142.3	251.1	9.79	52.39	0.57	5.35
SCB-3	139.5	152.1	258.8	9.19	38.26	0.59	4.16
SCB-4	121.5	136.3	237.6	7.75	45.17	0.57	5.83
SCB-5	135	153	254.7	10.16	50.41	0.6	4.96
SCB-6	135	142.6	242.1	10.63	39.58	0.59	3.72
SCB-7	135	153.6	262.8	10.82	56.3	0.58	5.2
SCB-8	103.5	120.3	216	9.96	36.17	0.56	3.63
SCB-9	112.5	139.7	261	6.27	39.49	0.54	6.3
SCB-10	135	151.2	252	6.16	36.92	0.6	5.99
SCB-11	135	123.5	255.6	10.65	48.05	0.48	4.51
SCB-12	112.5	146.3	257	8.21	76.56	0.57	9.32

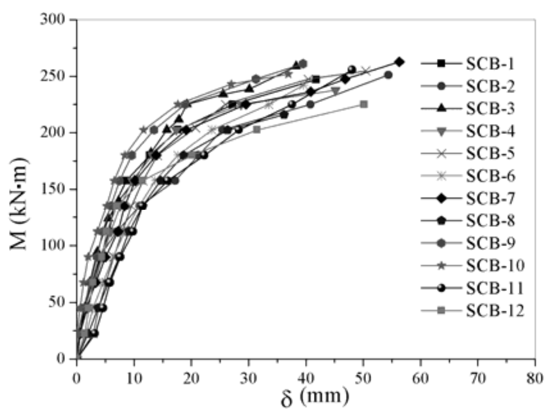

Figure 4. $M-\delta$ curve for specimens.

4.3 Strain Distributions across the Section

The research investigated the strain distributions along the depth of mid-span section for specimen SCB-1 and SCB-12. When the mid-span moment $M_t/M_{ut}\leq 0.54$, the strain of SCB-1 across section satisfied nearly linear distribution, which accorded well with the plain-section assumption. In plastic phase, however, strain along the depth of steel beam presented a fold-line distribution with the yielding of bottom flange. Meanwhile, the neutral axis which was located in the concrete slab moved upward gradually.

5 PARAMETRIC STUDY

Comparison between SCB-1, SCB-4, SCB-5 and SCB-6 showed that the support length of PPCRP had a significant impact on the flexural rigidity of composite beams in the elastic phase. Specimen SCB-1 with support length of 40 mm performed the highest flexural rigidity, which coincided well with the recommended support length onto the steel beam in the design handbook.

Experimental results about the composite floor slabs' thickness indicated that an increase in slab thickness led to an increase in flexural capacity. This was to be expected as an increase in the thickness would raise the neutral axis of the composite beam, hence increasing the lever arm of the section (Lam 2000). However, the specimen with the thicker slab didn't perform a higher flexural rigidity in the elastic phase.

When the degree of shear connection was lower than 1.0, a reduction in stud spacing caused both a significant improvement in flexural capacity and a decrease in mid-span deflection at the same load level. However, with the degree higher than 1.0, a reduction in stud spacing couldn't significantly improve the flexural capacity or rigidity.

In addition, changes in the longitudinal compressive reinforcement ratio contributed slightly to the flexural behavior of composite beams. It was observed that the composite beam with T-shaped ribs vertical to the steel beam had a higher rigidity but a close flexural capacity by comparison with the beam having ribs parallel to the steel beam.

6 CONCLUSIONS

This paper described an experimental study that focused on the flexural behavior of steel-concrete composite beam with composite floor slab comprising PPCRPs. At the collapse load, the specimens with composite floor slabs suffered a diagonal shear failure, due to the interface bond slip between the precast panel and the cast-in-situ layer. Compared with the floor slab cast in-situ, a slight decline in the ultimate flexural capacity was observed. Besides, the recommend support length was 40mm in the construction of floor slabs with PPCRPs. With the degree of shear connection lower than 1.0, a reduction in stud spacing could significantly improve the flexural capacity and rigidity.

References

Hegger, G., Shear capacity of prestressed hollow core slabs in slim floor constructions, *Engineering Structures*, 31(2), 551-559, Feb., 2009.

Lam, D., Parametric study on composite steel beams with precast concrete hollow core floor slabs, *Journal of Construction Steel Research*, 54(2), 283-304, May, 2000.

Lam, D., Capacities of headed stud shear connectors in composite steel beams with precast hollowcore slabs, *Journal of Constructional Steel Research*, 63(9), 1160-1174, Sept., 2007.

Wu, Fangbo, Experimental study and calculating methods on bending rigidity of precast prestressed concrete ribbed panels for composite slabs, *Journal of Hunan University (Natural Sciences)*, 38(4), 1-7, 2011.

Zhou, Xuhong, Design method of prestressed concrete simply supported on four sides of two-way composite slab, *Journal of Architecture and Civil Engineering*, 23(4), 54-57, 2006.